Ren-Gang Lv, Shu-Wen Chen* and Yan Gao*

A selective fluorescence probe based on benzothiazole for the detection of Cr^{3+}

https://doi.org/10.1515/hc-2017-0120
Received June 8, 2017; accepted July 10, 2017

Abstract: A novel benzothiazole-functionalized Schiff-base derivative **L** was prepared and its metal-ion sensing properties were investigated. Sensor **L** displays selective naked-eye color change from yellow to green in the presence of Cr^{3+} in aqueous solution at pH 7.2, while other cations do not interfere with the recognition of Cr^{3+}. The proposed mechanism is supported by Job's plot evaluation, IR and ESI-MS studies. The association constant and detection limit of sensor **L** to Cr^{3+} are 5.73×10^4 M^{-1} and 2.1×10^{-8} M, respectively. A B3LYP/6-31G (d,p) basis set was employed for optimization of **L** and **L**-Cr^{3+} complex.

Keywords: aqueous solution; benzothiazole; Cr^{3+}; naked-eye; recognition.

Introduction

Design and synthesis of fluorescent chemosensors capable of selective recognition of metal ions is an active field of research in supramolecular chemistry [1–4]. Among the metal ions, Cr^{3+} ion performs a crucial role in a wide range of biochemical processes, which is essential for good health in moderate intake; however, it is toxic at high concentration [5, 6]. Several biological functions depend directly or indirectly on the proper concentration and oxidation states of chromium to maintain the homoeostatic mechanism. Deficiency or overdose of chromium can lead to serious diseases, including Alzheimer's, Huntington's and Parkinson's disease [7, 8]. Ion recognition, particularly of toxic heavy metal ions is of intense interest as it has implications in the fields of environment, medicine and biology [9, 10]. Chemosensors for on-site selective and sensitive detection of such metal ions in aqueous phase is always endeavored. With the aid of suitable molecular probes, metal ions have been sensed in organic media, mixed organic solvents and aqueous-organic media [11–16]. There are reports in the literature for specific sensing of Cr^{3+} in aqueous solution using spectrophotometer, spectrofluorimeter and confocal microscope [17–23]. The potent toxicity of Cr^{3+} drives the need of simple, convenient and naked-eye visualization method for the detection in aqueous solution.

Recently, benzothiazole and Schiff base derivatives have become research hotspot in recognition of various analytes [24–29]. Here, we report a novel colorimetric chemosensor **L** based on a benzothiazole-functionalized Schiff-base derivative for the quantification of Cr^{3+} in aqueous solution. Ligand **L** specifically binds to Cr^{3+} in the presence of other competing cations with a substantial color change in HEPES buffer. This chemosensor provides a convenient and practical way to detect both Cr^{3+} in the environment.

Results and discussion

Compound **2** was synthesized by condensation of 2-formylbenzothiazole (**1**) and thiosemicarbazide in the refluxing acetic acid for 8 h. The unique ligand **L** was then obtained by condensation of **2** and 2-bromoacetophenone (Scheme 1). The molecular structure of **2** and **L** were confirmed by NMR, mass spectra and elemental analysis (see Figures S1, S2, S5–S8 in the online supplement).

Host-guest recognition experiments in aqueous DMSO, HEPES buffered solution, pH 7.2, were carried out. The coordination of **L** with Cr^{3+} was first investigated using UV-vis absorption spectroscopy. As shown in Figure 1, the addition of Cr^{3+} (10 μM) to **L** (5 μM) results in the spectral shift of the absorption peak from 378 nm to 589 nm along with color changes from yellow to green. Meanwhile, only slight absorption changes are induced by adding Cu^{2+}. In an analogous way, no significant adsorption and color changes occur in the presence of other metal ions including Fe^{3+}, Ag^{+}, Hg^{2+}, Co^{2+}, Ni^{2+}, Cd^{2+}, Pb^{2+}, Ba^{2+}, Mg^{2+}, Al^{3+}, Ca^{2+} and Zn^{2+}. This result indicates that **L** can serve as a 'naked-eye' Cr^{3+} indicator in aqueous media.

Additional studies of the Cr^{3+} – **L** complexation in HEPES buffer is shown in Figure 2. The initial absorption

---

***Corresponding authors: Shu-Wen Chen and Yan Gao,** School of Chemical Engineering, University of Science and Technology LiaoNing, Anshan 114051, China, e-mail: wangweisit@163.com (S.-W. Chen); gys20080901@163.com (Y. Gao)
Ren-Gang Lv: School of Chemical Engineering, University of Science and Technology LiaoNing, Anshan 114051, China

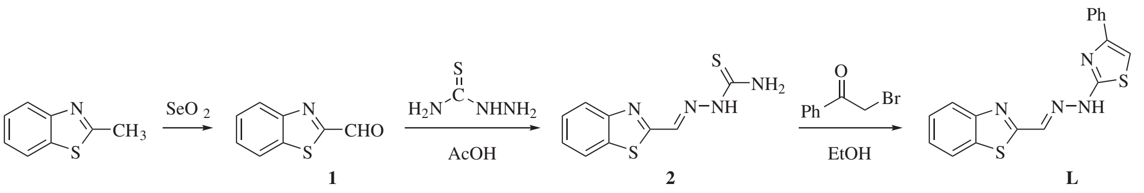

Scheme 1

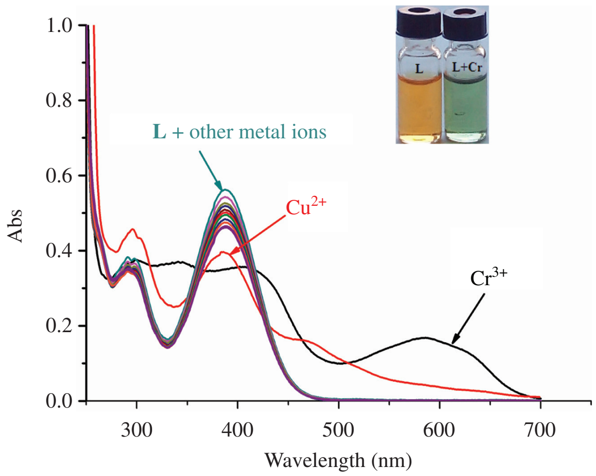

Figure 1 The absorption spectra of **L** (5 μM) in DMSO/H_2O solution (3:7, v/v; HEPES buffered, pH 7.2) upon addition of 2.0 equiv. of various metal ions.
Investigated metal ions are Cr^{3+}, Fe^{3+}, Ag^{+}, Cu^{2+}, Hg^{2+}, Co^{2+}, Ni^{2+}, Cd^{2+}, Pb^{2+}, Ba^{2+}, Mg^{2+}, Al^{3+}, Ca^{2+} and Zn^{2+}. Inset shows colors of **L** solution in the absence and presence of Cr^{3+} ion.

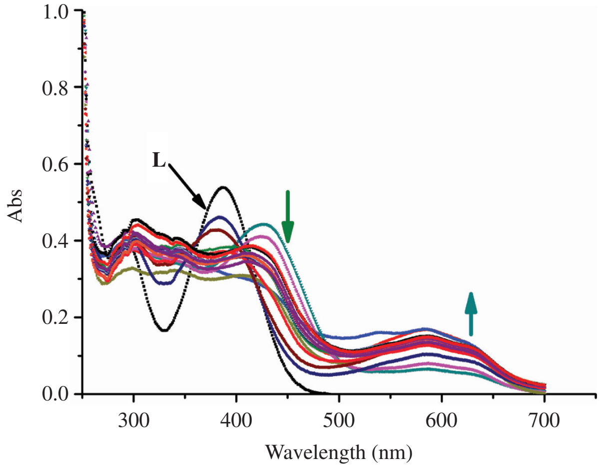

Figure 2 UV-vis absorption spectra of **L** (5 μM) in the presence of Cr^{3+} (0–15 μM) in DMSO/H_2O (3:7, v/v; HEPES buffered, pH 7.2).

maximum of **L** at 378 nm decreases upon gradual addition of Cr^{3+} ion with the concomitant appearance of a new absorption band at 426 nm. This new band also gradually decreases upon further addition of Cr^{3+} ion and a new peak at 589 nm gradually increases, implicating the formation of **L**-Cr^{3+} ensembles.

The fluorescence spectra ($\lambda_{ex}=358$ nm) of **L** in the absence and presence of various metal cations are shown in Figure 3. The sensor **L** shows a negligible fluorescence emission around 500 nm in the absence and presence of Fe^{3+}, Ag^{+}, Cu^{2+}, Hg^{2+}, Co^{2+}, Ni^{2+}, Cd^{2+}, Pb^{2+}, Ba^{2+}, Mg^{2+}, Al^{3+}, Ca^{2+} and Zn^{2+}. By contrast, the addition of Cr^{3+} creates a remarkable fluorescence enhancement at 536 nm. These results demonstrate that probe **L** shows an excellent selectivity toward Cr^{3+}.

Fluorescence titration experiments were also performed. As shown in Figure 4, upon incremental addition of Cr^{3+} (0–2.0 equiv.) to **L** solution, the fluorescence emission gradually increases and reaches the saturation state with 1.0 equiv. of Cr^{3+}. The nonlinear fit of the data reveals that the binding of **L** to Cr^{3+} is most probably of 1:1 stoichiometry. This binding mode is also supported by the data of Job's plots evaluated from the fluorescence spectra of **L** and Cr^{3+} with a total concentration of 20 μM (Figure S9). According to the linear Benesi-Hildebrand expression, the measured fluorescence intensity $[1/(F-F_0)]$ at 515 nm changes as a function of $1/[Cr^{3+}]$ in a linear relationship ($R^2=0.9962$). The association constant of **L** with Cr^{3+} in HEPES buffer was calculated to be 5.73×10^4 M^{-1}

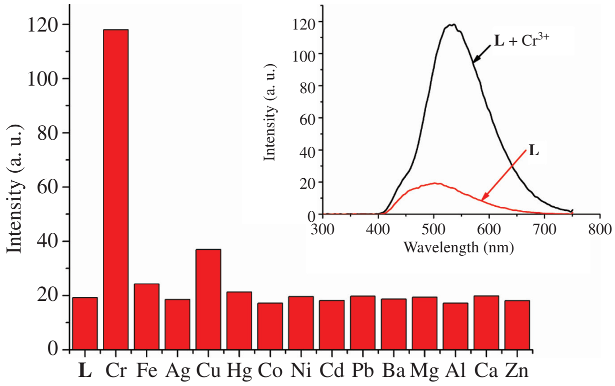

Figure 3 Fluorescence spectra of **L** (10 μM, $\lambda_{ex}=358$ nm) in the presence of different metal ions: Cr^{3+}, Fe^{3+}, Ag^{+}, Cu^{2+}, Hg^{2+}, Co^{2+}, Ni^{2+}, Cd^{2+}, Pb^{2+}, Ba^{2+}, Mg^{2+}, Al^{3+}, Ca^{2+} and Zn^{2+} (20 μM).

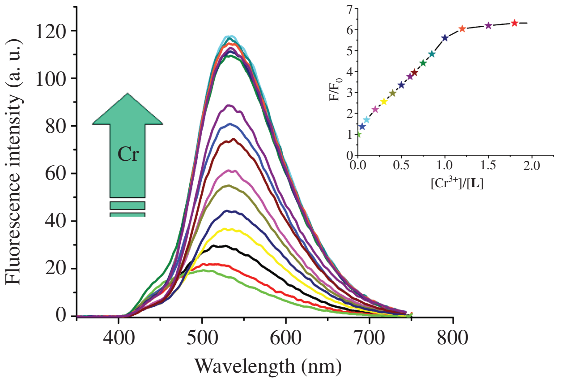

Figure 4 Fluorescence spectra of **L** (10 μм, pH 7.2) in buffered aqueous phase upon addition of increasing concentrations of Cr^{3+} (0–20 μм, $\lambda_{ex}=358$ nm).

(Figure S10). The detection limit for Cr^{3+} was estimated to be 2.1×10^{-8} м based on a 3σ/slope analysis under these experimental conditions (Figure S11). Furthermore, the fast fluorescence responses of **L** towards Cr^{3+} was also confirmed by the addition of Cr^{3+} (20 μм) to the solution of **L** (10 μм) in HEPES buffer. As shown in Figure S12, upon the addition of Cr^{3+}, a significant fluorescence response is observed within 5 min, indicating that the probe **L** could be used for the real-time detection of Cr^{3+}.

For the biological application of **L**, the sensing should operate in the physiological range of pH. As shown in Figure 5, the fluorescence intensity of **L** is stable in the pH range of 5–11. This result indicates that the probe **L** can be used as a chemosensor for Cr^{3+} detection under physiological conditions.

To check further the practical applicability of receptor **L** as a selective receptor, we carried out competition experiments (Figure 6). For the competition tests, receptor **L** was treated with 2 equiv. of Cr^{3+} and 2 equiv. of other metal ions such as Fe^{3+}, Ag^{+}, Cu^{2+}, Hg^{2+}, Co^{2+}, Ni^{2+}, Cd^{2+}, Pb^{2+}, Ba^{2+}, Mg^{2+}, Al^{3+}, Ca^{2+} and Zn^{2+}. No interference was observed for the detection of Cr^{3+} by **L** in aqueous solution under these conditions. These results indicate that **L** could be an excellent chromogenic sensor for Cr^{3+} over competing relevant metal ions in aqueous solution.

The green bars represent the emission changes of **L** in the presence of cations of interest (all are 20 μм). The red bars represent the changes of the emission that occurs upon the subsequent addition of 20 μм of Cr^{3+} to the solution.

The reversibility of the recognition process of **L** was analyzed by adding a bonding agent, Na$_2$EDTA. As shown in Figure 7, the addition of Na$_2$EDTA to a mixture of **L** and

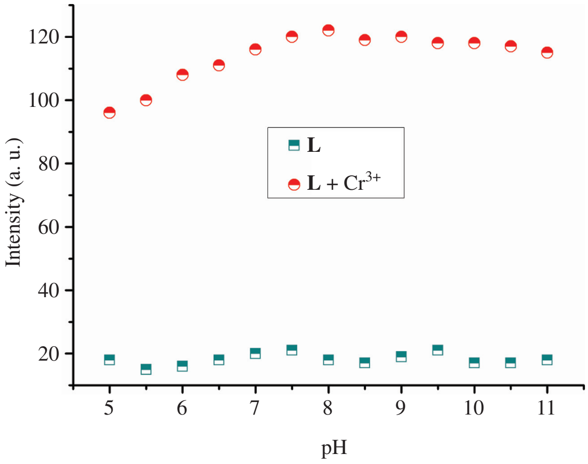

Figure 5 The effect of pH (5.0–11.0) on the fluorescence intensity of **L** (10 μм) with 2.0 equiv. Cr^{3+} in DMSO/H$_2$O solution (3:7, v/v; HEPES buffered, pH 7.2).

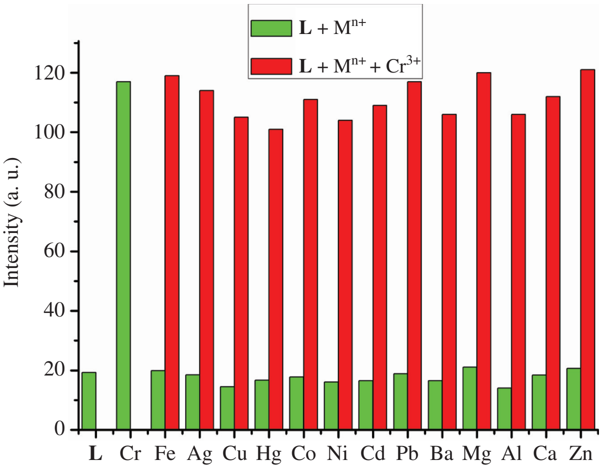

Figure 6 Relative fluorescence intensity of **L** (10 μм) in the presence of various cations in DMSO/H$_2$O solution (3:7, v/v; HEPES buffered, pH 7.2, $\lambda_{ex}=358$ nm).

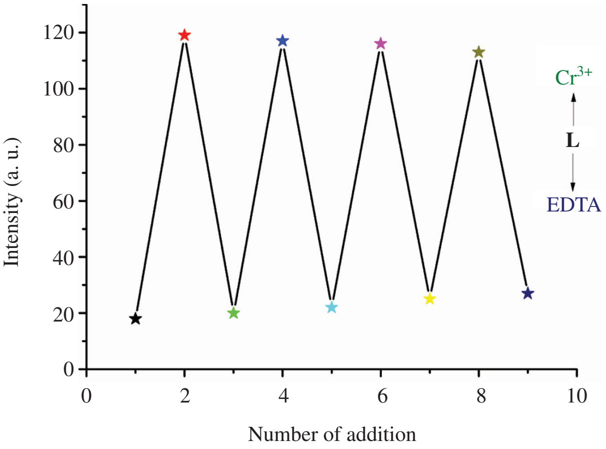

Figure 7 Fluorescence responses of **L** (10 μм) after the sequential addition of Cr^{3+} and EDTA.

Cr^{3+} results in the decrease of the fluorescence intensity, which indicates the regeneration of the free sensor **L**. It means that the receptor **L** could be used as a selective fluorescent sensor for detection and recognition of Cr^{3+} in such fields of environmental analysis.

To verify the potential application of the fluorescent sensor **L**, the Cr^{3+} determination in tap and bottled water samples was conducted using the fluorescence spectroscopy. The results were calculated by linear equation and are listed in Table 1. All measurements were repeated three times. As can be seen, the recovery of Cr^{3+} in all determined water samples ranges from 96.7 to 104.8% and the relative standard deviation (RSD) is under 1.83%. These data demonstrate that the present probe can be used for the practical detection of Cr^{3+} in aqueous samples in the presence of potentially competing metal ion species.

The recognition mechanism of the sensor **L** with Cr^{3+} was investigated by using mass and infrared spectra. The mass spectrum obtained in the presence of sodium ion shows a molecular-ion peak $[\mathbf{L}+Na^+]^+$ at *m/z* 359.03931. When Cr^{3+} ion is added into the solution of **L**, the resultant peak at *m/z* 458.95294 is assignable to $[\mathbf{L}+Cr^{3+}+2Cl^-]^+$ species (Figure S3). We studied the IR spectra of free ligand **L** and the complex **L**-Cr^{3+} again and the results are shown in Figure S4. Upon addition of Cr^{3+} to **L**, the IR spectrum of **L** undergoes changes with the vibrational frequency of CH=N undergoing a red shift from 1636 cm^{-1} to 1653 cm^{-1}. This result suggests that the nitrogen atom of CH=N may participate in binding with Cr^{3+}. The IR frequency of N-H undergoes a blue shift from 3182 cm^{-1} to 3169 cm^{-1}, which can be attributed to the change of chemical environment near the N-H moiety. In addition, the slight change of aromatic frequency can be attributed to the coordination of the nitrogen of thiazole with Cr^{3+}. Therefore, the observed differences in the IR spectra of **L** in the absence and presence of Cr^{3+}, coupled with ESI-MS analysis and Job's plot analysis, are consistent with the proposed chelation as shown in Scheme 2. The **L**-Cr^{3+} interactions may involve the imine nitrogen and the nitrogen of the thiazole group to forms a 1:1 complex (Scheme 2).

Table 1 Analytical results of Cr^{3+} in water samples ($n=3$).

Samples	Added (μM)	Found[a] (μM)	Recovery (%)	RSD[b] (%)
Bottled water	10.0	9.87	98.7	0.29
	50.0	48.36	96.7	0.36
	100.0	98.74	98.7	0.45
Tap water	10.0	10.48	104.8	0.52
	50.0	50.93	101.9	0.84
	100.0	99.55	99.6	1.67

[a]Mean value from three determinations. [b]Relative standard deviation from three determinations.

To better understand the nature of the coordination of Cr^{3+} with **L**, energy-optimized structures of **L** and its corresponding complexes with Cr3$^+$ were obtained using density functional theory (DFT) calculations at the B3LYP/6-31G(d) level using Lanl2dz basis set for simple receptor **L** and **L**-Cr^{3+} complex. The spatial distributions and orbital energies of the highest occupied molecular orbital (HOMO) and the lowest unoccupied molecular orbital (LUMO) of **L** and the corresponding metal complexes were also calculated. As shown in Figure 8, the HOMO is distributed on the whole molecule in **L**, whereas LUMO is distributed on the benzothiazole ring in **L**. Meanwhile, the π electrons of HOMO of **L**-Cr^{3+} is mainly distributed on the chromium and the benzothiazole. The LUMO is distributed on the chromium and the corresponding coordination site in **L**-Cr^{3+}. The energy gaps between the HOMO and LUMO in the **L** and **L**-Cr^{3+} were calculated to be 3.50210 eV and 2.34834 eV, respectively, indicating that the binding of Cr^{3+} to **L** decreases the HOMO-LUMO energy gap of the complex and stabilizes the system. Thus, these results are consistent with a favorable complexation according to the proposed coordination.

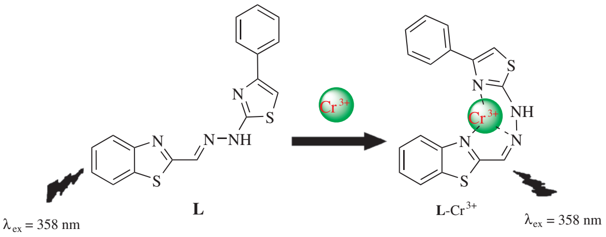

Scheme 2 Proposed mechanism for Cr^{3+} chelation by **L**.

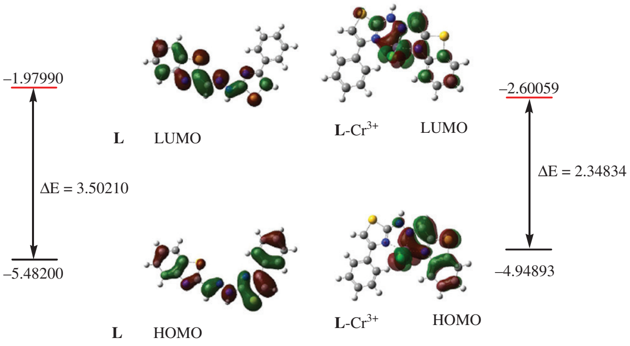

Figure 8 Energy diagram of HOMO and LUMO orbital **L** and **L**-Cr^{3+} complex.

Conclusion

A new benzothiazole-based fluorescent chemosensor **L** for Cr^{3+} detection in mixed aqueous medium (DMSO/H_2O solution, 3:7, HEPES buffered, pH = 7.2) was developed. The experimental results clearly indicate that compound **L** is a highly sensitive and selective chemosensor for Cr^{3+}. The receptor selectivity and sensitivity are not affected in the presence of other metal ions. According to Job's plot, a 1:1 stoichiometry complex between **L** and Cr^{3+} is formed. This excellent selectivity suggests a potential application of the chemosensor in the biological monitoring and tracking of Cr^{3+}. A B3LYP/6-31G (d,p) basis set was employed for optimization of **L** and **L**-Cr^{3+} complex.

Experimental

2-Formylbenzothiazole [30] was prepared as reported previously. All chemicals were commercially available, and the organic solvents were dried over appropriate drying agents and distilled prior to use. Double-distilled water was used. Salts of metal ions Ca^{2+}, Mg^{2+}, Ni^{2+}, Co^{2+}, Zn^{2+}, Cu^{2+}, Hg^{2+}, Pb^{2+}, Fe^{3+}, Ba^{2+}, Ag^{+}, Al^{3+}, Cr^{3+} and Cd^{2+} were used to evaluate the probe selectivity. ^{1}H NMR spectra (500 MHz) and ^{13}C NMR spectra (125 MHz) were recorded on a Bruker AV 500 spectrometer using DMSO-d_6 as solvent. ESI mass spectra were recorded on a Bruker Solarix 70 high-resolution instrument. Elemental analyses were performed on a Perkin-Elmer 240 analyzer. The UV-vis and fluorescence experiments were performed on a Lambda-900 spectrometer and a Perkin-Elmer LS-55 fluorescence spectrophotometer, respectively.

Synthesis of 2

A mixture of 2-formylbenzothiazole (5 mmol), thiosemicarbazide (5 mmol), glacial acetic acid (3 mL) and ethanol (20 mL) was magnetically stirred at reflux until the reaction was completed, as monitored by TLC. The resulting precipitate of **2** was collected and purified by silica gel column chromatography eluting with petroleum ether/ethyl acetate, 9:1 to afford 0.87 g (74%); ^{1}H NMR: δ 11.96 (s, 1H, NH), 8.61 (s, 1H, CH=N), 8.37 (s, 1H, NH), 8.12 (d, J = 7.9 Hz, 1H, Ar), 8.06–7.95 (m, 2H, NH, Ar), 7.54 (t, J = 7.6 Hz, 1H, Ar), 7.49 (t, J = 7.6 Hz, 1H, Ar); ^{13}C NMR: δ 179.0, 164.9, 153.7, 137.2, 134.6, 127.0, 126.8, 123.5, 122.8. ESI-MS. Calcd for $C_9H_8N_4S_2$: *m/z* 236.3163. Found: *m/z* 237.02601 (M + H$^+$). Anal. Calcd for: C, 45.74; H, 3.41; N, 23.71. Found: C, 45.79; H, 3.38; N, 23.66.

Synthesis of L

A mixture of **1** (5 mmol), 2-bromoacetophenone (5 mmol) and acetic acid (30 mL) was magnetically stirred at reflux until the reaction was completed as monitored by TLC. The resultant precipitate of **L** was filtered and purified by silica gel column chromatography eluting with petroleum ether/ethyl acetate, 7:3 to afford compound **L** as an orange solid: yield 0.99 g (59%); IR: *ν* 3182, 3062, 1636, 1587, 1480, 1457, 783 cm^{-1}; ^{1}H NMR: δ 12.90 (s, 1H, NH), 8.30 (s, 1H, CH=N), 8.11 (d, J = 7.9 Hz, 1H, Ar), 8.00 (d, J = 8.1 Hz, 1H, Ar), 7.88 (d, J = 7.6 Hz, 2H, Ar), 7.61–7.39 (m, 5H, Ar), 7.33 (t, J = 7.2 Hz, 1H, Ar); ^{13}C NMR: δ 167.3, 165.3, 153.8, 151.3, 135.6, 134.2, 129.2, 128.3, 127.0, 126.6, 126.0, 123.4, 122.8, 105.6. ESI-MS. Calcd for $C_{17}H_{12}N_4S_2$: *m/z* 336.4335. Found: *m/z* 359.03931 (M + Na$^+$). Anal. Calcd for: C, 60.69; H, 3.59; N, 16.65. Found: C, 60.74; H, 3.57; N, 16.61.

Recognition studies

The metal binding studies were performed in 10-mL volumetric flasks with fixed concentration of metal ion (0.2 mM) along with compound **L** (0.1 mM) in HEPES buffered solution (50 mM, pH 7.2). The titration experiments were conducted manually by stepwise addition of Cr^{3+} to the buffered solution of compound **L** (10 mL). To guarantee the uniformity of solution, enough time was given before recording any spectrum. The association constant was calculated according to the equation of Benesi-Hildebrand [31]. The stoichiometry of compound **L** and Cr^{3+} was determined by Job's method from the fluorescence data [32]. For fluorescence intensity measurements, the excitation wavelength was fixed at 358 nm. The slit widths were 10 nm/10 nm.

Association constant calculation

For the formation of a 1:1 complex between the chemosensor **L** and cation Cr^{3+}, the following Benesi-Hildebrand equation was used:

$$\frac{1}{F-F_0}=\frac{1}{K_a(F_{max}-F_0)[Cr^{3+}]}+\frac{1}{F_{max}-F_0}$$

where F and F_0 represent the fluorescence emission of **L** in the presence and absence of Cr^{3+}, respectively, F_{max} is the saturated emission of **L** in the presence of excess amount of Cr^{3+}; $[Cr^{3+}]$ is the concentration of Cr^{3+} ion added, and K_a is the binding constant.

Acknowledgments: This work was supported by the financial support of the Key Laboratory Project of Liaoning Province (2008S127).

References

[1] Chandrasekhar, V.; Das, S.; Yadav, R.; Hossain, S.; Parihar, R.; Subramaniam, G.; Sen, P. Novel chemosensor for the visual detection of copper(II) in aqueous solution at the ppm level. *Inorg. Chem*. **2012**, *51*, 8664–8666.

[2] Zhao, B.; Ruan, Y. Y.; Deng, Q. G.; Wang, L. Y.; Song, B.; Feng, Y. Q. Synthesis and characterization of heteroarylthio derivatives of 5,17-di-*tert*-butyl-11,23-diamido-25,27-diprotected calix[4] arene. *Heterocycl. Commun*. **2013**, *1*, 327–329.

[3] Qu, W. J.; Guan, J.; Wei, T. B.; Yan, G. T.; Lin, Q.; Zhang, Y. M. A turn-on fluorescent sensor for relay recognition of two ions: from a F^--selective sensor to highly Zn^{2+}-selective sensor by tuning electronic effects. *RSC. Adv*. **2016**, *6*, 35804–35808.

[4] Lin, Q.; Lu, T. T.; Zhu, X.; Wei, T. B.; Li, H.; Zhang, Y. M. Rationally introduced multi-competitive binding interactions in supramolecular gels: a simple and efficient approach to develop multi-analyte sensor array. *Chem. Sci*. **2016**, *7*, 5341–5346.

[5] Vincent, J. B. Quest for the molecular mechanism of chromium action and its relationship to diabetes. *Nutr. Rev*. **2000**, *58*, 67–72.

[6] Eastmond, D. A.; MacGregor, J. T.; Slesinski, R. S. Trivalent chromium: assessing the genotoxic risk of an essential trace element and widely used human and animal nutritional supplement. *Crit. Rev. Toxicol*. **2008**, *38*, 173–190.

[7] Liu, D.; Pang, T.; Ma, K.; Jiang, W.; Bao, X. A new highly sensitive and selective fluorescence chemosensor for Cr^{3+} based on rhodamine B and a 4,13-diaza-18-crown-6-ether conjugate. *RSC. Adv*. **2014**, *4*, 2563–2567.

[8] Lei, Y.; Su, Y.; Huo, J. Photophysical property of rhodamine-cored poly(amidoamine)dendrimers: simultaneous effect of spirolactam ring-opening and PET process on sensing trivalent chromium ion. *J. Lumin*. **2011**, *131*, 2521–2527.

[9] Li, X.; Gao, X.; Shi, W.; Ma, A. H. Design strategies for water-soluble small molecular chromogenic and fluorogenic probes. *Chem. Rev*. **2014**, *114*, 590–659.

[10] Espinosa, A.; Otón, F.; Martínez, R.; Tárraga, A.; Molina, P. A multidimensional undergraduate experiment for easy solution and surface sensing of mercury(II) and copper(II) metal cations. *J. Chem. Edu*. **2013**, *90*, 1057–1060.

[11] Han, Y.; You, Y.; Lee, Y. M.; Nam, W. Double Action: toward phosphorescence ratiometric sensing of chromium ion. *Adv. Mater*. **2012**, *24*, 2748–2754.

[12] Kim, H. N.; Ren, W. X.; Kim, J. S.; Yoon, J. Fluorescent and colorimetric sensors for detection of lead, cadmium, and mercury ions. *Chem. Soc. Rev.* **2012**, *41*, 3210–3244.

[13] Xua, Z.; Zhang, L.; Guo, R.; Xiang, T.; Wu, C.; Zheng, Z.; Yang, F. A highly sensitive and selective colorimetric and off-on fluorescent hemosensor for Cu^{2+} based on rhodamine B derivative. *Sens. Actuators B*. **2011**, *156*, 546–552.

[14] Kim, H.; Wang, S.; Kim, S. H.; Son, Y. A. Design, synthesis and optical property of rhodamine 6G based new dye sensor. *Mol. Cryst. Liq. Cryst*. **2012**, *566*, 45–53.

[15] Bag, B.; Pal, A. Rhodamine-based probes for metal ion-induced chromo-/fluorogenic dual signaling and their selectivity towards Hg (II) ion. *Org. Biomol. Chem*. **2011**, *9*, 4467–4480.

[16] Venkateswarulu, M.; Sinha, S.; Mathew, J.; Koner, R. R. Quencher displacement strategy for recognition of trivalent cations through 'turn-on' fluorescence signaling of an amino acid hybrid. *Tetrahedron. Lett.* **2013**, *54*, 4683–4688.

[17] Saha, S.; Mahato, P.; Reddy, U. G.; Suresh, E.; Chakrabarty, A.; Baidya, M.; Ghosh, S. K.; Das, A. Recognition of Hg^{2+} and Cr^{3+} in physiological conditions by a rhodamine derivative and its application as a reagent for cell-imaging studies. *Inorg. Chem*. **2012**, *51*, 336–345.

[18] Wang, J. N.; Qi, Q.; Zhang, L.; Li, S. H. Turn-on luminescent sensing of metal cations via quencher displacement: rational design of a highly selective chemosensor for chromium(III). *Inorg. Chem*. **2012**, *51*, 13103–13107.

[19] Zhou, Y.; Zhang, J.; Zhang, L.; Zhang, Q.; Ma, T.; Niu, J. A rhodamine-based fluorescent enhancement chemosensor for the detection of Cr^{3+} in aqueous media. *Dyes Pigments* **2013**, *97*, 148–154.

[20] Elavarasi, M.; Rajeshwari, A.; Chandrasekaran, N.; Mukherjee, A. Simple colorimetric detection of Cr(III) in aqueous solutions by as synthesized citrate capped gold nanoparticles and development of a paper based assay. *Anal. Methods* **2013**, *5*, 6211–6218.

[21] Zhao, M.; Ma, L.; Zhang, M.; Cao, W.; Yang, L.; Ma, L. J. Glutaminecontaining "turn-on" fluorescence sensor for the highly sensitive and selective detection of chromium (III) ion in water. *Spectrochim. Acta. A. Mol. Biomol. Spectrosc*. **2013**, *116*, 460–465.

[22] Shyamaprosad, G.; Avijit, K. D.; Anup, K. M.; Abhishek, M.; Krishnendu, A.; Sibaprasad, M.; Partha, S.; Tarun, K. M. Visual and near IR (NIR) fluorescence detection of Cr^{3+} in aqueous media via spirobenzopyran ring opening with application in logic gate and bio-imaging. *Dalton Trans*. **2014**, *43*, 231–239.

[23] Sima, P.; Abhishek, M.; Shyamaprosad, G. A differentially selective molecular probe for detection of trivalent ions (Al^{3+}, Cr^{3+} and Fe^{3+}) upon single excitation in mixed aqueous medium. *Dalton Trans*. **2015**, *44*, 11805–11810.

[24] Wang, L. N.; Qin, W. W.; Liu, W. S. A sensitive Schiff-base fluorescent indicator for the detection of Zn^{2+}. *Inorg. Chem. Commun*. **2010**, *13*, 1122–1125.

[25] Abhishek, M.; Shyamaprosad, G. Ratiometric detection of hypochlorite applying the restriction to 2-way ESIPT: simple design for ''naked-eye'' tap water analysis. *New J. Chem*. **2015**, *39*, 4424–4429.

[26] Li, G. B.; Fang, H. C.; Cai, Y. P.; Zhou, Z. Y.; Thallapally, P. K.; Tian, J. Construction of a Novel Zn-Ni Trinuclear Schiff Base and a Ni^{2+} Chemosensor. *Inorg. Chem*. **2010**, *49*, 7241–7243.

[27] Shyamaprosad, G.; Abhishek, M.; Monalisa, M.; Debasish, S. Cascade reaction-based rapid and ratiometric detection of H_2S/S^{2-} in the presence of bio-thiols with live cell imaging: demasking of ESIPT approach. *RSC Adv*. **2014**, *4*, 62639–62643.

[28] Shyamaprosad, G.; Abhishek, M.; Sima, P.; Anup, K. M.; Partha, S.; Ching, K. Q.; Fun, H. K. FRET based 'red-switch' for Al^{3+} over ESIPT based 'green-switch' for Zn^{2+}: dual channel detection with live-cell imaging on a dyad platform. *RSC Adv*. **2014**, *4*, 34572–34576.

[29] Shymaprosad, G.; Manna, A.; Paul, S.; Das, A. K.; Aich, K.; Nandi, P. K. Resonance-assisted hydrogen bonding induced nucleophilic addition to hamper ESIPT: ratiometric detection of cyanide in aqueous media. *Chem. Commun*. **2013**, *49*, 2912–2914.

[30] Zubarovskii, V.; Briks, Yu. Reaction of 2-acetylbenzothiazole with 2-formylbenzothiazole. *Chem. Heterocycl. Compd*. **1982**, *18*, 485–488.

[31] Benesi, H. A.; Hildebrand, J. H. A spectrophotometric investigation of the interaction of iodine with aromatic hydrocarbons. *J. Am. Chem. Soc*. **1949**, *71*, 2703–2707.

[32] Job, P. Formation and stability of inorganic complexes in solution. *Ann. Chim*. **1928**, *9*, 113–203.

Supplemental Material: The online version of this article offers supplementary material (https://doi.org/10.1515/hc-2017-0120).